Electronic Supplementary Information

for

Synthesis and crystal structures of Mn(II) and Co(II) complexes as catalysts for oxidation of cyclohexanone

Adedibu C. Tella [1,2,*], Aaron Y. Isaac [1,3], Hadley S. Clayton [2], Adeniyi S. Ogunlaja [4], Aswathy T. Venugopalan [3,5], Marimuthu Prabu[3,5] and Raja Thirumalaiswamy [3,5]

[1] Department of Chemistry, University of Ilorin, P.M.B. 1515, Ilorin, 24003, Kwara State, Nigeria; aaryone1@gmail.com
[2] Department of Chemistry, University of South Africa, Unisa 0003, South Africa; clayths@unisa.ac.za
[3] Inorganic Chemistry and Catalysis Division, CSIR-National Chemical Laboratory, Dr. Homi Bhabha Road, Pune 411008, India; tv.aswathy@ncl.res.in (A.T.V.); m.prabu@ncl.res.in (P.M.); t.raja@ncl.res.in (R.T.)
[4] Department of Chemistry, Nelson Mandela University, P.O. Box 77000, Port Elizabeth 6031, South Africa; adeniyi.ogunlaja@mandela.ac.za
[5] Academy of Scientific and Innovative Research (AcSIR), CSIR-HRDC Campus, Ghaziabad 201002, UP, India
* Correspondence: ac_tella@yahoo.co.uk Tel.: +234-803-501-9197

Supplementary Information Table of Contents

Table S1: Selected FTIR spectra data of [Mn(2,6-pydc)$_2$](imi) **(1)** and its ligands

Compound	νC-N *str.*	νC=O *str.*	νC-O *str.*	νOH	νCOO *sym.*	νCOO *asym.*	Δ νCOO *sym.*	νM-O	νM-N
imi	1295s	-	-	-	-	-	-	-	
2,6-pydc	1181s	1706s	1256w	3212w	-	-	-	-	
1	1319s	1692s	1394s	-	1456ms	1312s	164	663s	578b

Table S2: Selected data of FTIR spectra of [Co(H_2pza)$_2$(H_2O)$_2$(NO_3)].NO_3 **(2)** and its ligand

Compound	νC-N *str.*	$\nu_{sy}/\nu_{say}NH_2$	νOH_w	νC=O *str.*	νM-O	νM-N
H_2pza	1253s	3301ms	3285ms	1708s	-	-
2	1190s	-	-	1684s	782s	675s

NB: w = water

Table S3: Selected data of the electronic spectra of 1 and its ligands

Compound	E, cm^{-1} (λ_{max}, nm)	Assignments
imi	35714 (280)	$\pi \rightarrow \pi^*$ / $n \rightarrow \pi^*$
2,6-pydc	43478 (230); 36101 (277)	$\pi \rightarrow \pi^*$ / $n \rightarrow \pi^*$
1	31545 (317); 14556 (687)	LMCT, $^4T_{1g}$ (G) $\leftarrow$ $^6A_{1g}$

λ_{max} = absorption maxima; E = energy of electronic transition

Table S4: Selected data of the UV-Visible spectra of 2 and its ligand

Compound	E, cm^{-1} (λ_{max}, nm)	Assignments
H_2pza	45248 (221); 38461 (260); 31645 (316)	$\pi \rightarrow \pi^*$ / $n \rightarrow \pi^*$
2	30030 (333); 19047 (525)	LMCT, $^4A_{2g} \rightarrow {}^4T_{1g}$ (P)

λ_{max} = absorption maxima; E = energy of electronic transition

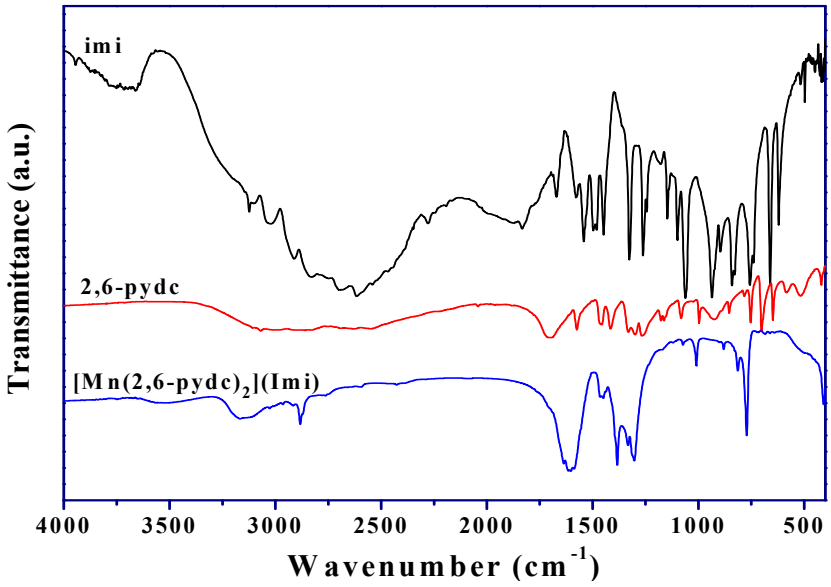

Figure S1: FTIR spectra of [Mn(2,6-pydc)$_2$](imi) (1) and its ligands

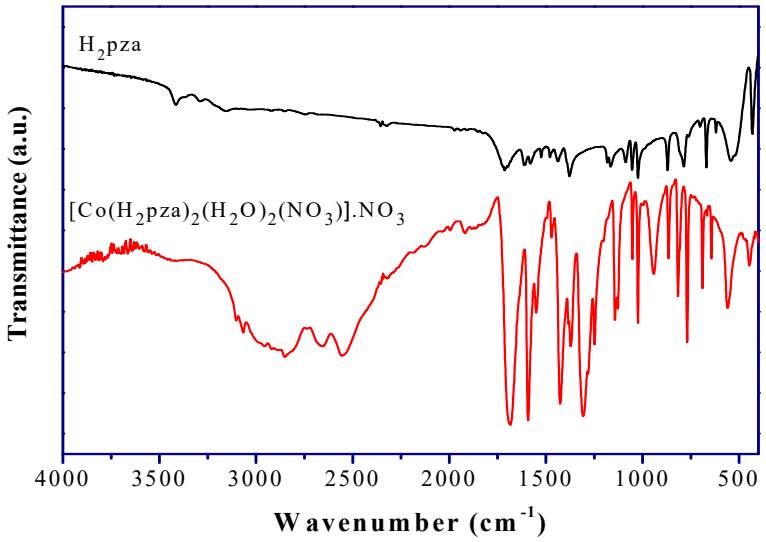

Figure S2: FTIR spectra for [Co(H$_2$pza)$_2$(H$_2$O)$_2$(NO$_3$)]•NO$_3$ (2)

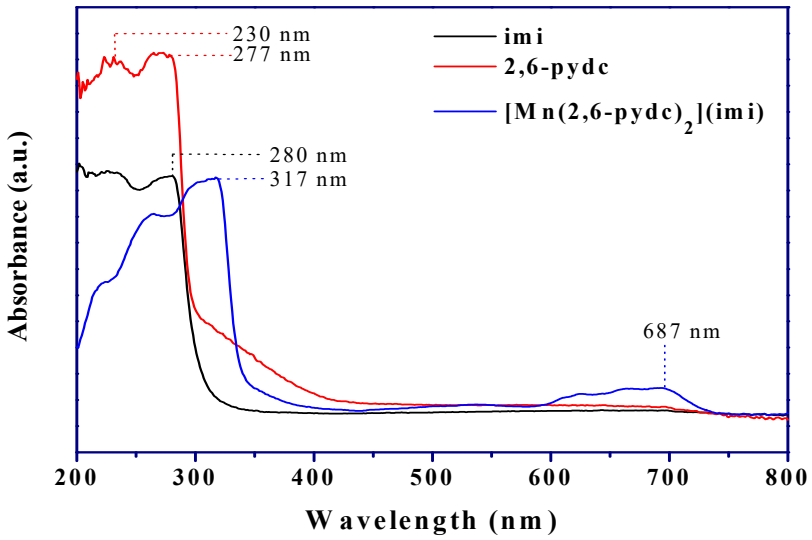

Figure S3: UV-Vis. spectra of **1** and its ligands

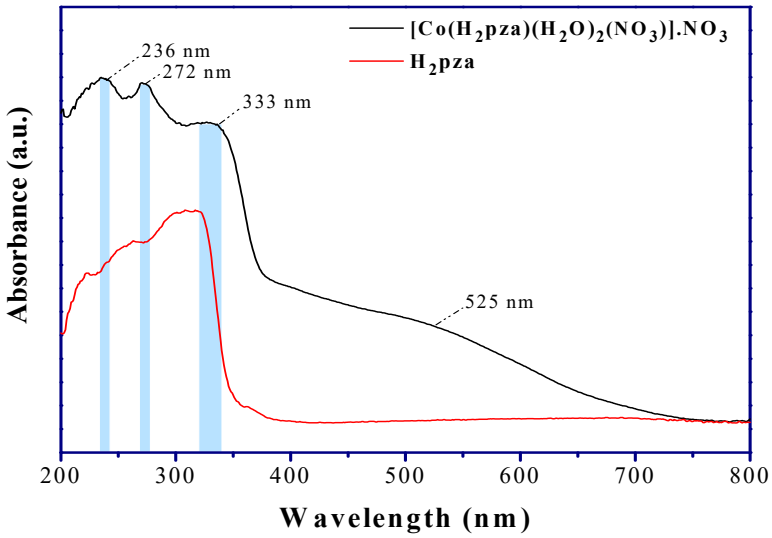

Figure S4: UV-Visible spectra of **2** and its ligand

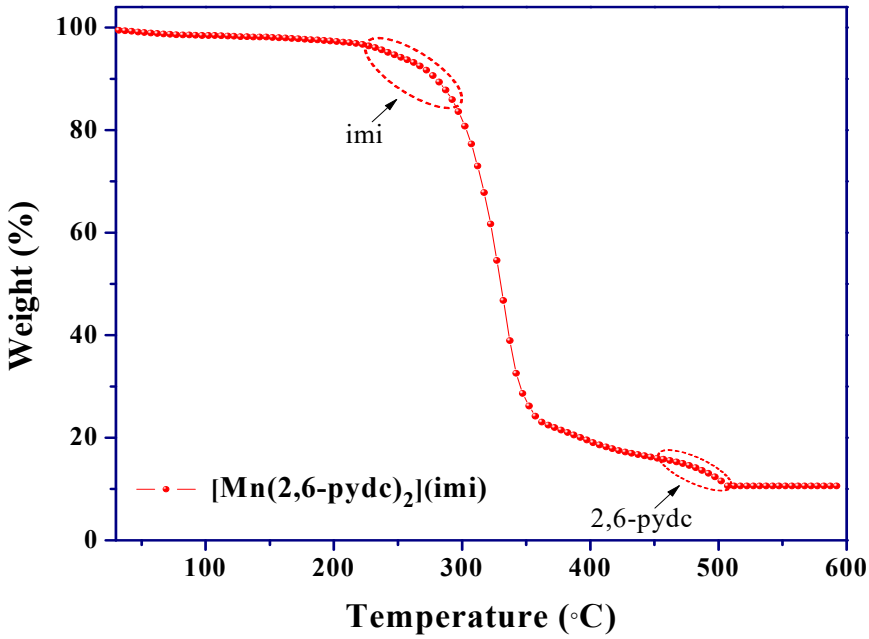

Figure S5: TGA curve of **1**

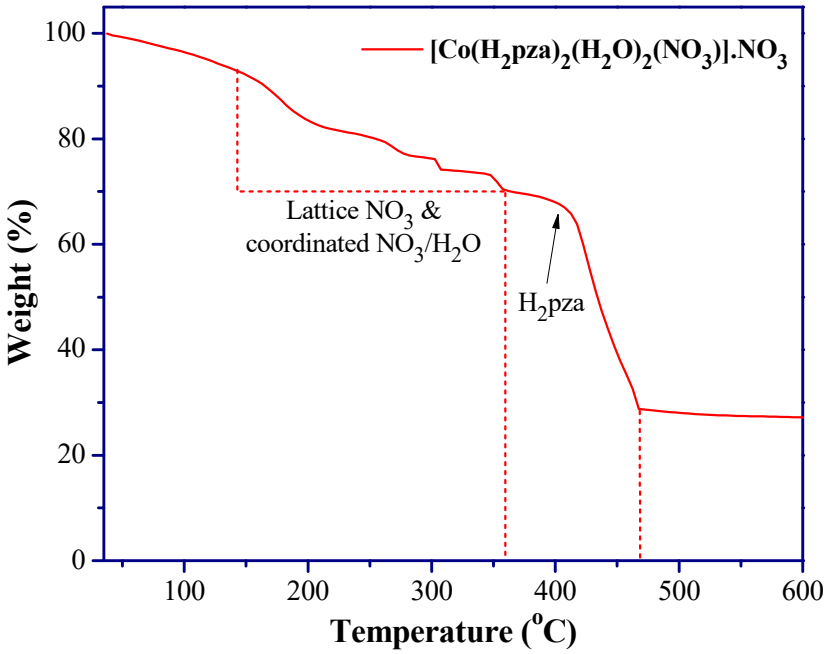

Figure S6: TG curve of **2**

X-ray Crystallography of [Mn(2,6-pydc)$_2$](imi) (1) and [Co(H$_2$pza)$_2$(H$_2$O)$_2$(NO$_3$)]•NO$_3$ (2)

X-ray crystallographic data collection for **1** and **2** were carried out on a Super Nova Dual X-ray Diffractometer system (Agilent Technologies) and Bruker Kappa Apex II Duo diffractometer (Madison, Wisconsin), respectively. The temperatures of scans for **1** and **2** were maintained at 100K and 298 K, respectively. Hydrogen atoms, (C-H/O-H = 0.95 Å/0.84 Å) for **1** and (C-H = 0.93 Å) for **2** were included on each refined structures as riding atoms. The crystal data collection and structure refinement parameters of **1** and **2** are highlighted in Tables S5 below.

Table S5: The crystal data collection and structure refinement parameters for the cocrystals (**1a**) and crystals of **1** and **2**.

Compound identification	(2,6-pydc–imi$^+$)(1a)	[Mn(2,6- pydc)$_2$](imi) (1)	Co(H$_2$pza)$_2$(H$_2$O)$_2$(NO$_3$)]•NO$_3$ (2)
Empirical formula	$C_{10}H_9N_3O_4$	$C_{17}H_{10}MnN_4O_8$	$C_{10}H_{14}CoN_8O_{10}$
Formula weight	235.20	453.23	465.22
Crystal system	Orthorhombic	Orthorhombic	Triclinic
Temperature(K)	100(2)	298(2)	100(2)
Space group	$P2_12_12_1$	Pbca	P-1
a(Å)	3.7272(1)	7.7662(3)	6.9057(3)
b(Å)	14.4056(5)	15.2799(6)	9.1738(3)
c(Å)	18.4364(7)	12.4110(9)	14.1486(5)
α(°)	90	90	90.6490(10)
β(°)	90	90	98.6600(10)
γ(°)	90	90	102.0680(10)
V(Å^3)	989.90(6)	3442.7(2)	865.683(6)
Z	4	8	2
D_c (g/mm^3)	1.5781	1.7487	1.785
μ(mm^{-1})	0.125	0.827	1.066
F(000)	488.3	1835.8	474.0
h,k,l ranges	-6+5, -19+21, -23+29	±10, -12+20, -39+34	±9, ±13, ±20
Reflections	9042	12759	61970
R_{int}	0.0637	0.0396	0.0338

Data/restraints/parameters	8112/0/618	4073/0/270	5284/4/272
Goodness-of-fit on F^2	1.022	1.559	1.116
R_1 [I> 2σ (I)]	0.0482	0.0723	0.0387
wR_2 (all data)	0.1326	0.2250	0.1099
Max/min. (e Å^3)	0.35/-0.31	1.86/-0.73	0.66/-1.17
Colour/shape	Grey/flake	Colourless/block	Pink/block

Table S6: Selected hydrogen bond parameters for **1**

D----H···A	D---H (Å)	D···A (Å)	H···A (Å)	D---H···A (°)
N3---H3a----O3	0.860	2.789	1.942	168.32

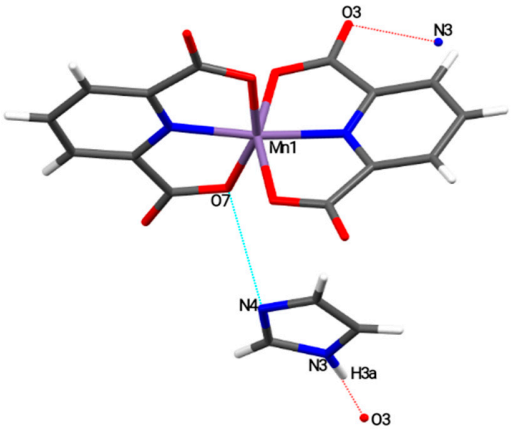

Figure S7: 2D view of compound **1** [010] showing HB interactions between pydc and (imi).

The selected bond distances and angles of **1** are presented in Table S7.

Table S7: Selected bond lengths (Å) and angles (°) for 1

Bond distances (Å)		*Bond angles (°)*	
Mn1-O5	2.023(3)	O2-Mn1-O5	91.46(15)
Mn1-O2	2.000(3)	O4-Mn1-O5	91.99(14)
Mn1-O4	2.011(3)	O4-Mn1-O2	157.91(12)
Mn1-O7	1.998(3)	O7-Mn1-O5	157.68(13)
Mn1-N2	1.957(3)	O7-Mn1-O2	93.69(14)
Mn1-N1	1.971(3)	O7-Mn1-O4	91.34(13)
		N2-Mn1-O5	78.60(14)
		N2-Mn1-O2	101.35(14)
		N2-Mn1-O4	100.72(13)
		N2-Mn1-O7	79.09(13)
		N1-Mn1-O5	91.14(14)
		N1-Mn1-O2	79.41(14)
		N1-Mn1-O4	78.71(13)
		N1-Mn1-O7	111.16(14)
		N1-Mn1-N2	169.71(14)

Symmetry codes: x, y, z; -x, -y –z; ½+x, ½-y,-z; -x, ½+y, ½-z, ½-x, -y, ½+z, ½-x, ½+y, z; x, ½-y, +z; ½+x, y, ½-z

Table S8: Selected bond distance (Å) and angles (°) for **2**

Bond distances (Å)		Bond angles (°)	
Co1-O7	2.1197(14)	O7-Co1-O2	97.57(6)
Co1-O2	2.1591(14)	O7-Co1-O6	169.47(5)
Co1-O6	2.1604(14)	O2-Co1-O6	92.88(5)
Co1-O3	2.3481(15)	O7-Co1-O3	85.39(5)
Co1-N4	2.3570(16)	O2-Co1-O3	162.30(5)
Co1-N1	2.3613(15)	O6-Co1-O3	84.25 (5)
O10-N8	1.247(2)	O7-Co1-N4	92.90(6)
O8-N8	1.263(2)	O2-Co1-N4	72.00(5)
O3-N7	1.271(2)	O6-Co1-N4	91.55(6)
O9-N8	1.248(2)	O3-Co1-N4	125.44(5)
O4-N7	1.225(2)	O7-Co1-N1	92.58(6)
O5-N7	1.247(2)	O2-Co1-N1	82.18(5)
		O6-Co1-N1	87.55(5)
		O3-Co1-N1	80.26(5)
		N4-Co1-N1	154.09(5)
		N7-O3-Co1	102.83(11)
		O4-N7-O5	122.59(12)
		O4-N7-O3	120.55(11)
		O10-N8-O8	119.84(16)
		O9-N8-O8	119.28(16)

Symmetry codes: x, y, z; -x, -y, -z

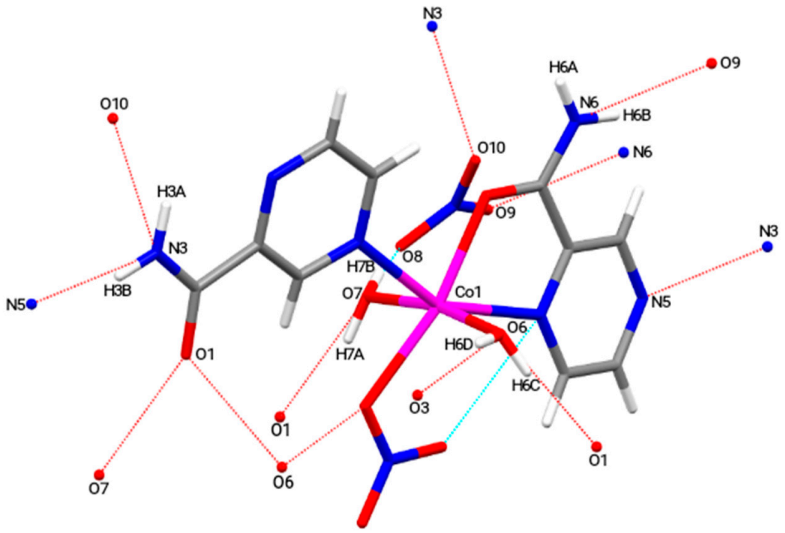

Figure S8: 1D view of **2** [100] showing network of hydrogen bonds

Table S9: Selected hydrogen bond parameters for **2**

D—H---A	D---H (Å)	D----A (Å)	H-----A (Å)	D---H-----A (°)
N3---H3A--------N5	0.880	2.990	3.376	57.11
N3--H3B----------N5	0.880	2.990	2.138	163.56
N3---H3A--------O10	0.880	2.833	2.134	135.89
N3--H3B----------O10	0.880	2.833	2.951	73.71
O6---H6C----------O1	0.840	2.706	1.876	169.88
O6--H6D----------O1	0.796	2.706	3.025	59.26
O6---H6C----------O3	0.840	2.858	2.086	65.01
O6---H6D----------O3	0.796	2.858	3.109	163.39
O7---H7----------O1	0.840	2.739	1.926	162.61
O7---H7B----------O1	0.797	2.739	3.160	51.74
O7---H7A----------O8	0.840	2.674	2.977	61.09
O7---H7B----------O8	0.797	2.674	1.902	162.69
N6----H6A---------O9	0.880	2.894	3.195	62.36
N6---H6B----------O9	0.880	2.894	2.084	152.69

Symmetry codes: x, y, z; -x, -y, -z

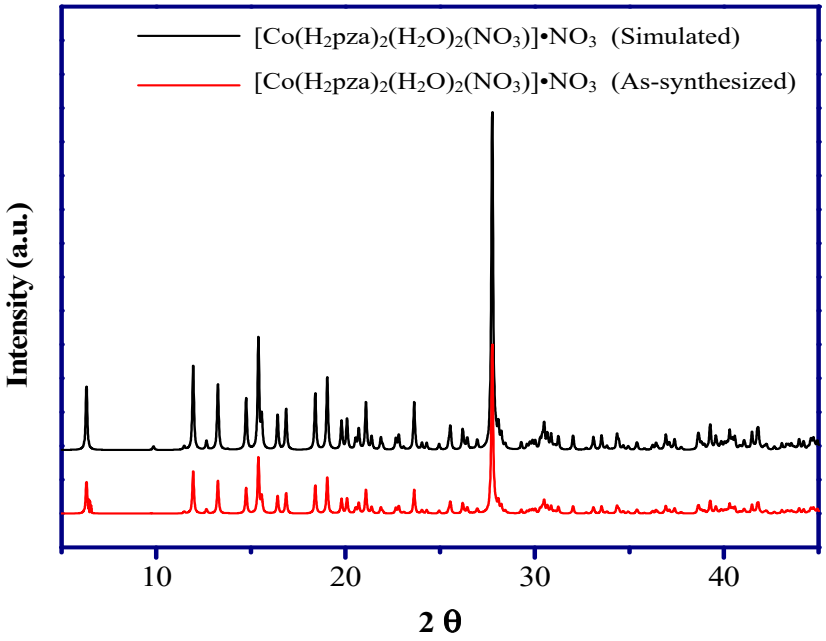

Figure S9: PXRD patterns (Cu, Kα) of simulated and crushed samples of compound **1**

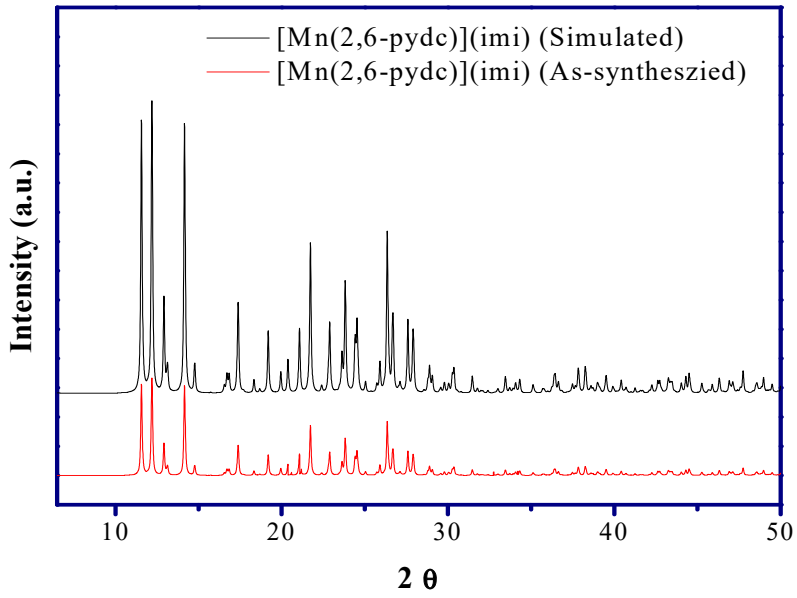

Figure S10: PXRD patterns (Cu, Kα) of simulated and crushed samples of compound **2**

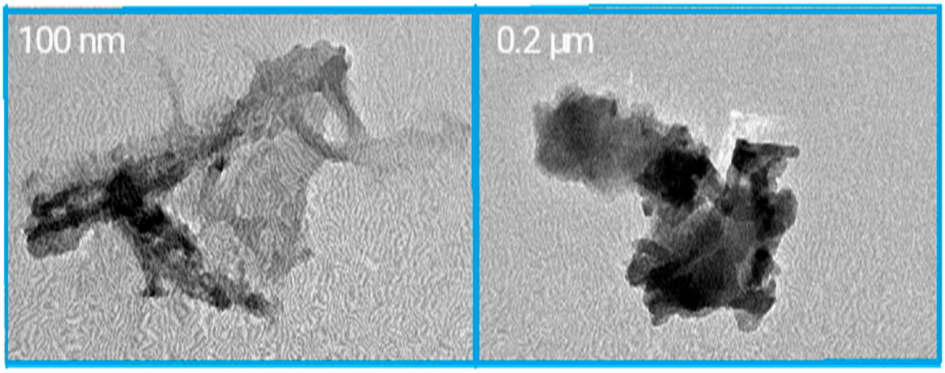

Figure S11A: High resolution TEM images of **1** viewed at 100 nm and 0.2 µm magnification.

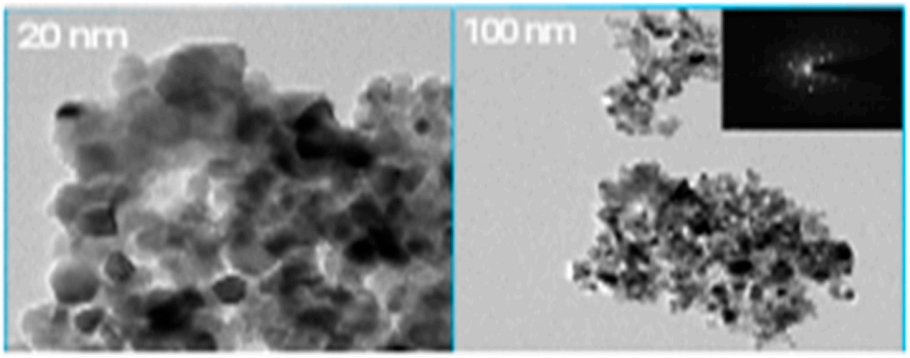

Figure S11B: The high resolution TEM images of **2** scanned at 20 nm and 100 nm magnification; inset represents the SAED of **2**.

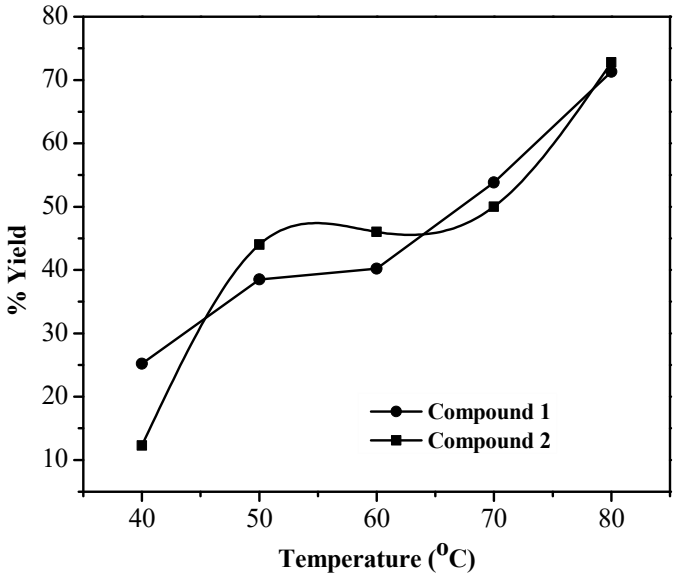

Figure S12: The effect of reaction temperature on the oxidation of cyclohexanone. Reaction conditions: Compound 1 (0.0029 mol L^{-1}), 1ml of 0.0394 wt% cyclohexanone in CH_3CN /water, 2 hrs, 4 ml H_2O_2 (30% aqueous, 170.4 mmol); compound 2 (0.0021 mol L^{-1}), 1ml of 0.0394 wt% cyclohexanone in CH_3CN /water, 3 hrs, 4 ml H_2O_2 (30% aqueous, 170.4 mmol).

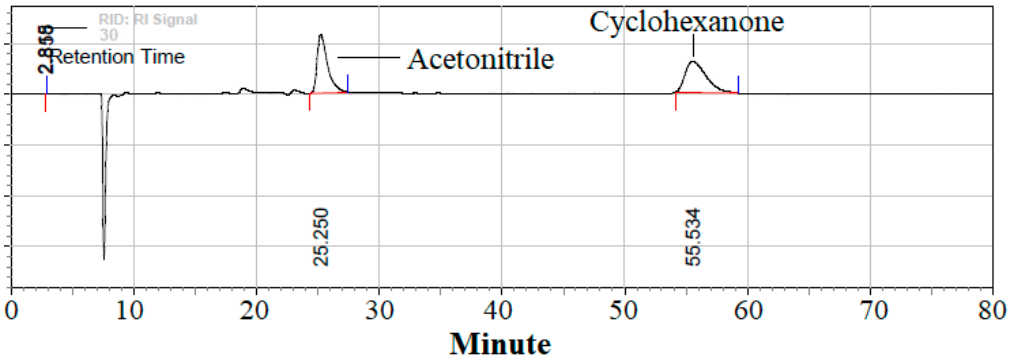

Figure S13: HPLC chromatogram of an aliquot (2µL) taken after oxidation of cyclohexanone in the absence of compound **1** which we ascribed to no yield promoting effect. Reaction conditions: 1 ml of cyclohexanone (0.0394 wt%), 4 ml of H_2O_2 (30% aqueous, 170.4 mmol)

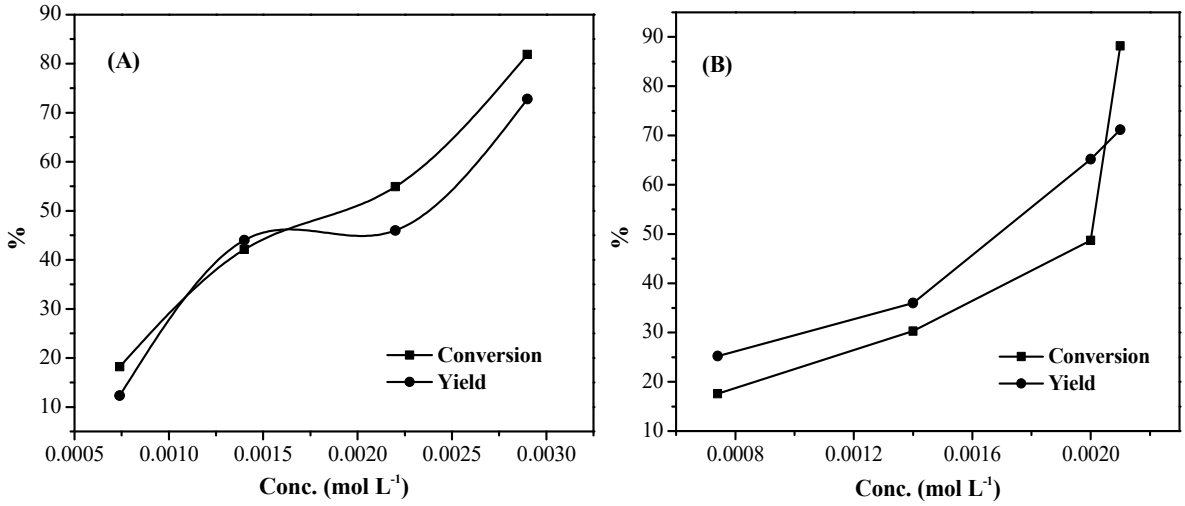

Figure S14: The effect of catalysts loading on the oxidation of cyclohexanone; (A) Reaction conditions: Compound 1 (optimum 0.0029 mol L^{-1}), 1ml of 0.0394 wt% cyclohexanone in CH_3CN /water, 2 hrs, 4 ml H_2O_2 (30% aqueous, 170.4 mmol); (B) compound 2 (optimum 0.0021 mol L^{-1}), 1ml of 0.0394 wt% cyclohexanone in CH_3CN /water, 3 hrs, 4 ml H_2O_2 (30% aqueous, 170.4 mmol).

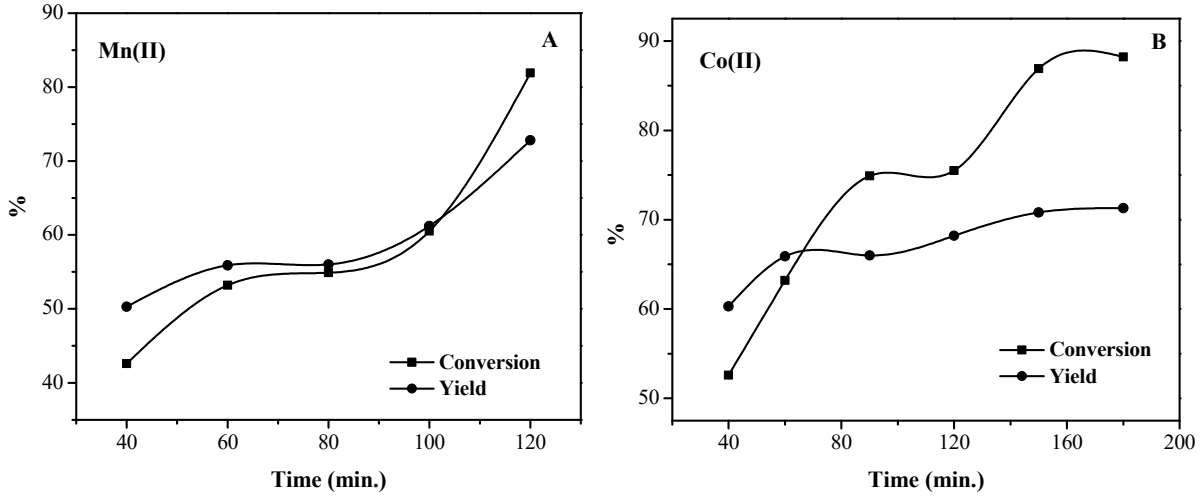

Figure S15 A: The effect of reaction time on the oxidation of cyclohexanone; (Mn^{2+} catalyst) Reaction conditions: Catalyst amount (optimum 0.0029 mol L^{-1}), 1ml of 0.0394 wt% cyclohexanone in CH_3CN /water, 2 hrs, 4 ml H_2O_2 (30% aqueous, 170.4 mmol); Figure 15 B: The effect of reaction time on the oxidation of cyclohexanone; (Co^{2+} catalyst) Reaction conditions: Catalyst amount (optimum 0.0021 mol L^{-1}), 1ml of 0.0394 wt% cyclohexanone in CH_3CN /water, 3 hrs, 4 ml H_2O_2 (30% aqueous, 170.4 mmol).

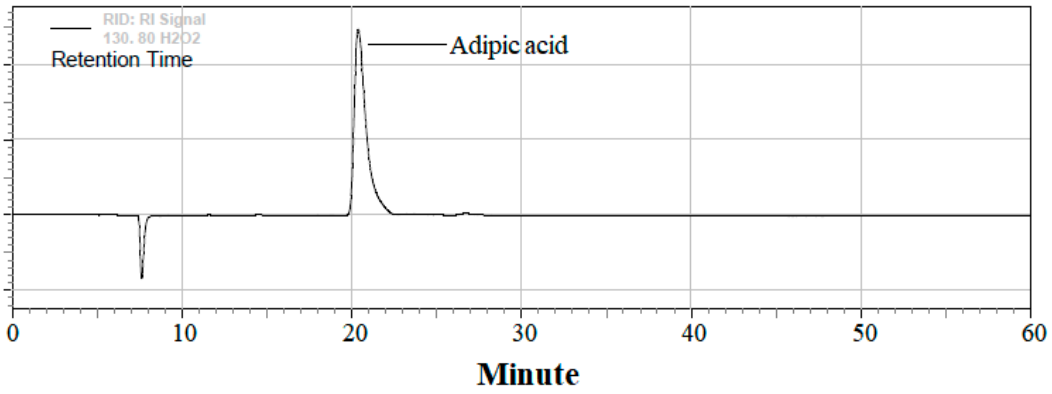

Figure S16: HPLC chromatogram of an aliquot of target product, [Table 2, Entry 5]. Reaction conditions: compound **1** (2.9×10^{-3} mol L^{-1}), 1ml of 0.0394 wt% cyclohexanone in CH_3CN /water, 2 hrs with **1**, 4 ml H_2O_2 (30% aqueous, 170.4 mmol).

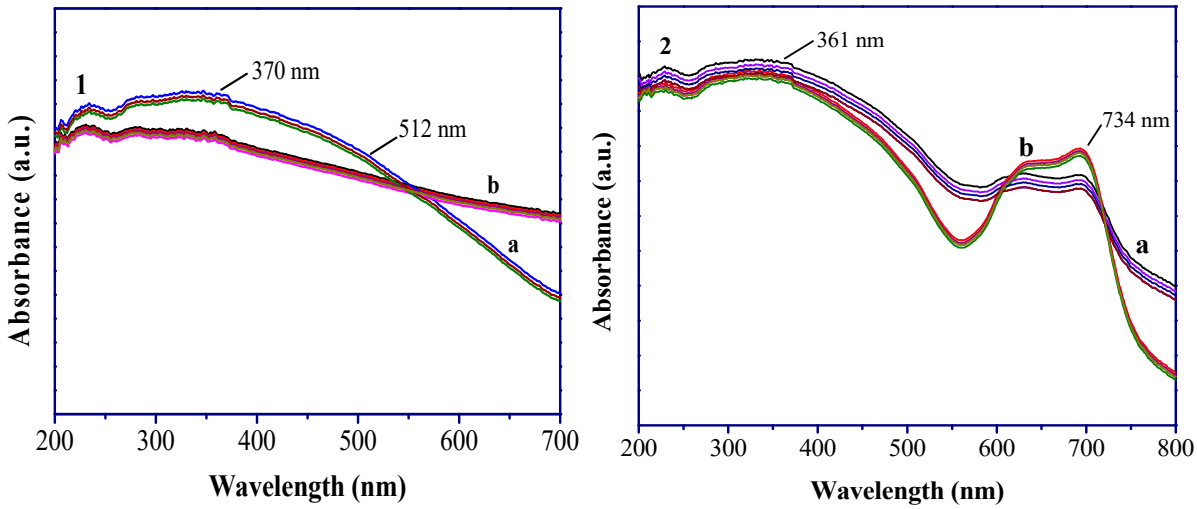

Figure S17: UV-Visible spectra studies of (1a) $[Mn(2,6\text{-}pydc)_2](imi)$ and cyclohexanone; (1b) $[Mn(2,6\text{-}pydc)_2](imi)$, cyclohexanone, and H_2O_2; (2a) $[Co(H_2pza)_2(H_2O)_2(NO_3)]\bullet NO_3$, and cyclohexanone; (2b) $[Co(H_2pza)_2(H_2O)_2(NO_3)]\bullet NO_3$, cyclohexanone, and H_2O_2. NB: Solvent in which experiment was performed is acetronitrile and there was an increase in the d-d band region as the reaction progresses in reaction systems containing **1** and **2**.

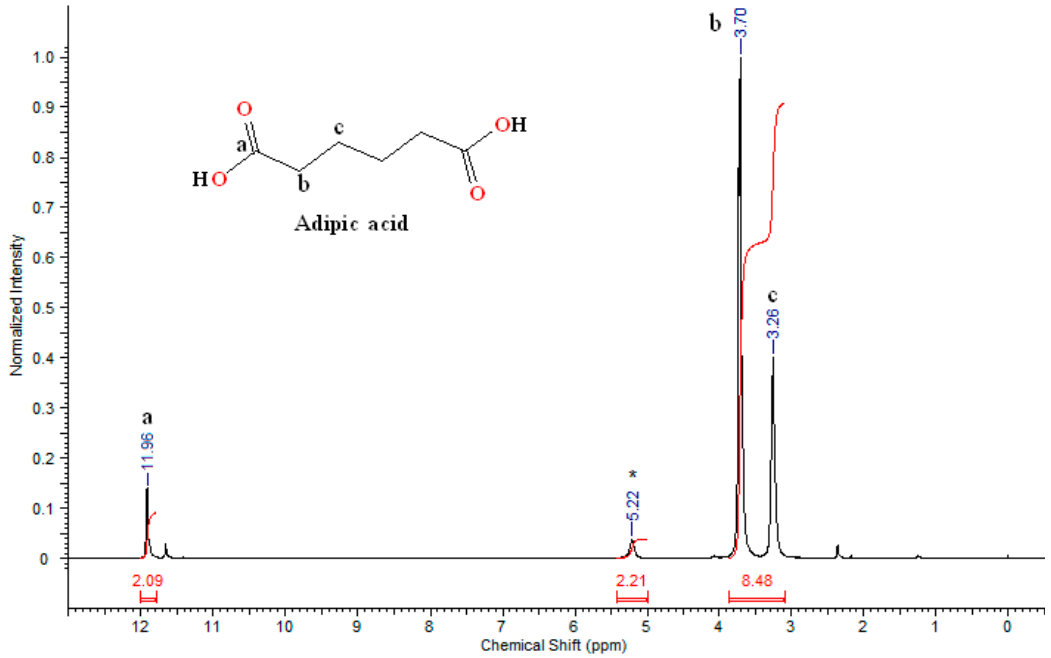

Figure S18: [1]H NMR spectrum (DMSO-D6) of the isolated adipic acid obtained with compound **1**

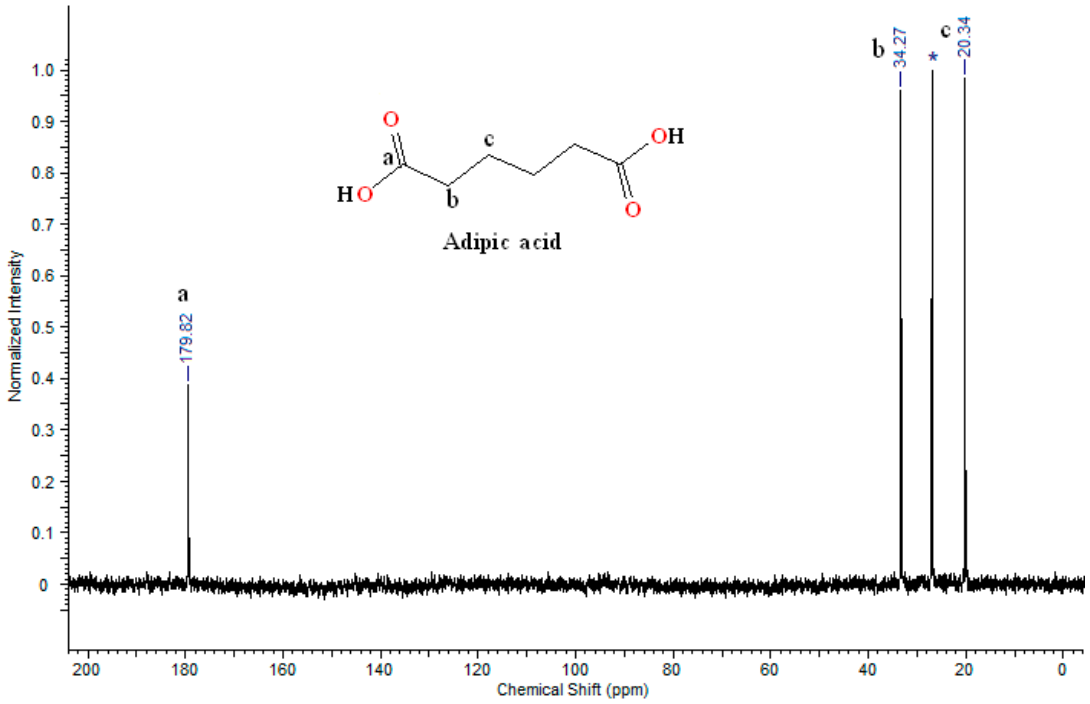

Figure S19: [13]C NMR spectrum (DMSO-D6) of the isolated adipic acid obtained with compound **1**

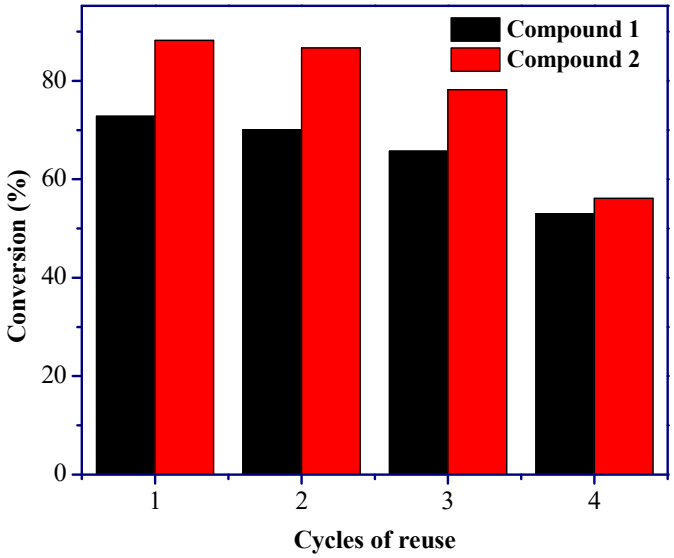

Figure S20: Illustration for the catalytic activities of compounds **1** and **2**

Cyclohexanone oxidation: Considering that the reaction proceeds as this: $A_C \leftrightarrow 2B_i \rightarrow C_P$; where, A_C = concentration of reactant (e.g. cyclohexanone), $2B_i$ = intermediate products, and C_P = concentration of the target product, then, the conversions (%) of cyclohexanone were calculated using equation below:

$$\text{Conversion (\%)} = \frac{Co - Cf}{Co} \times 100\%$$

Where C_o is the initial moles of cyclohexanone and, C_f is the final moles of cyclohexanone converted.

The selectivity (%) of adipic acid was calculated using equation below:

$$\text{Selectivity (\%)} = \frac{Amount\ of\ adipic\ acid\ produced}{Conversion} \times 100\%$$

The yield (%) of adipic acid was calculated using equation below:

$$\text{Yield (\%)} = \frac{Total\ moles\ of\ adipic\ acid\ produced}{Initial\ moles\ of\ cyclohexanone} \times 100\%$$

To study the kinetics and thermodynamics of the reaction, different concentrations, 6.4 x 10^{-4} mol L^{-1}; 7.7 x 10^{-4} mol L^{-1}; 9.0 x 10^{-4} mol L^{-1}; 1.03 x 10^{-3} mol L^{-1}; and 1.2 x 10^{-3} mol L^{-1} of cyclohexanone were prepared by dissolving varying amounts, 1.0 mL, 1.2 mL, 1.4 mL, 1.6 mL, and 1.8 mL of cyclohexanone in each reaction system. The total volume of each reaction system was 24 mL and contains 0.0394wt% of cyclohexanone.

Kinetics and thermodynamics of the catalytic oxidation of cyclohexanone

The kinetic studies of the catalytic oxidation of cyclohexanone over compounds **1** and **2** were carried out by using Langmuir-Hinshelwood (L-H) mechanism of a unimolecular reaction which is described as follows (Kumar *et al*, 2008):

$$A + S \underset{K_{-1}\ (Desorption)}{\overset{K_1\ (Adsorption)}{\rightleftharpoons}} AS \xrightarrow{K_2\ (Decomposition)} Product$$

By applying steady state approximation, the rate of reaction for the above mechanism becomes:

$$r = \frac{d[AS]}{dt} = k_1[A][S] - k_{-1}[AS] - k_2[AS] = 0$$

The L-H rate law for the first order unimolecular reaction can be expressed as:

$$\frac{1}{r} = \frac{1}{K_1[A]} + \frac{K_{-1}}{k_1 K_2}$$

Where, r = rate of reaction, [A] = final concentration of cyclohexanone, k_1 = adsorption rate constant, k_{-1}, desorption rate constant, and k_2 = decomposition rate constant. The slope and intercept corresponds to the above rate constants, and can be obtained in a L-H linear plot of 1/r vs. 1/[A]. The L-H plot for the oxidation of cyclohexanone is shown in Fig. S21.

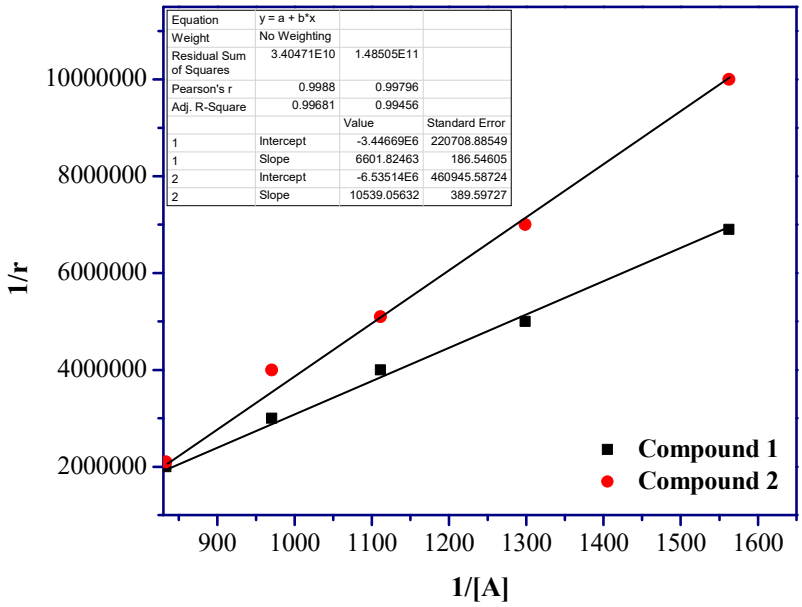

Figure S21: The L-H plot for the oxidation of cyclohexanone

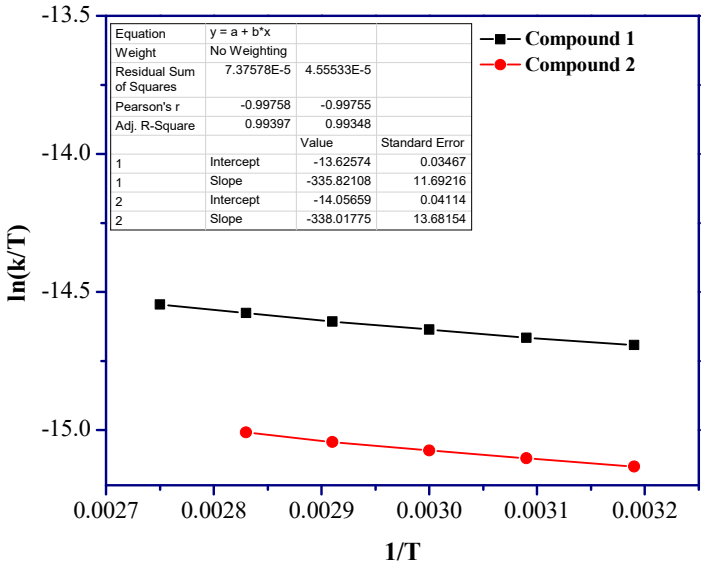

Figure S22: Arrhenius and Eyring plot of cyclohexanone oxidation over compounds **1** and **2**

References

38. K. V. Kumar, K. Porkodi, F. Rocha. (2008): "Langmuir–Hinshelwood kinetics – A theoretical study" *Catalysis Communications*, 9, 82–84.
39. R. I. Masel (2001) *"Chemical Kinetics and Catalysis" Wiley-Interscience,* New York, ISBN 0-471-24197-0